ORGANOMETALLICS

Article

pubs.acs.org/Organometallics

Agostic versus Terminal Ethyl Rhodium Complexes: A Combined Experimental and Theoretical Study

Ana M. Geer,[†] José A. López, Miguel A. Ciriano, and Cristina Tejel*

Departamento Química Inorgánica, Instituto de Síntesis Química y Catálisis Homogénea (ISQCH), CSIC-Universidad de Zaragoza, Pedro Cerbuna 12, 50009-Zaragoza, Spain

Supporting Information

ABSTRACT: Ethylene insertion into Rh−H bonds in complexes bearing an anionic *fac*-triphosphane ligand gives hydrido complexes, *β*-agostic species, or noninteracting ethyl derivatives depending on the reaction conditions. Several chemical equilibria between these species have been analyzed by NMR and DFT calculations, which revealed that they are mainly controlled by the entropy. Moreover, *β*-agostic species were found to be lower in enthalpy than the corresponding hydride−ethylene complexes, probably due to the steric pressure exerted by the bulky *fac*-triphosphane ligand.

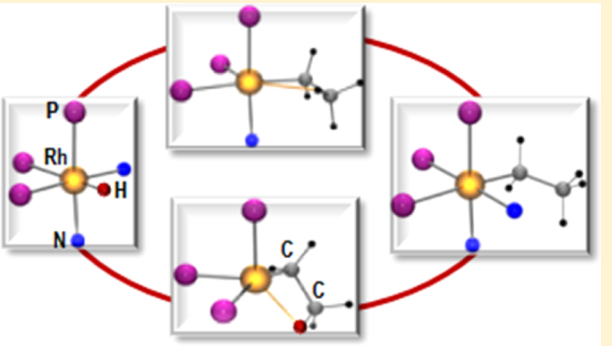

INTRODUCTION

Weak interactions between nonpolar C−H bonds and transition metals have been proved to be of paramount importance in organometallic chemistry and catalysis, contributing to major developments in the field of C−H bond activation and/or functionalization processes,[1] as well as in dehydrogenation reactions.[2] Both versions, intermolecular (*σ*-complexes) and intramolecular (agostic[3] complexes) are known, the latter being important intermediates connecting two fundamental reactions in organometallic chemistry, namely, the insertion of olefins into M−H bonds and the reverse one, the *β*-hydrogen elimination. Nowadays, the significance of agostic species becomes evident from the large body of literature in which the multiple roles they can play is enlightened.[4] As a way of example, *α*-agostic interactions have been proved to have a strong impact on the stereospecificity and rate of olefin insertion in polymerization;[5] *β*-agostic species often lead to C−H activation reactions,[6] while the *γ*-agostic ones have been reported to be crucial in the stabilization of the propagating species in vinyl norbornene polymerization.[7] Moreover, a delicate balance between electronic versus steric factors can tip the stability of *α*- versus *β*-agostic compounds,[8] or even between *β*- and *γ*-agostomers.[9] Furthermore, longer range interactions such as the rare *δ*- and *ε*-agostic ones are involved in uncommon intramolecular 1,4-, metal migration or 1,5-*σ* bond metathesis, respectively.[10] In other instances, they are valuable intermediates connecting the transition states that lead to C−H versus C−C activation reactions,[11] and also documented is their participation in the stabilization of highly unsaturated intermediates—such as T-shaped d^8-ML_3 complexes[12]—requiring two agostic interactions in some cases.[13]

A key feature of these particular M−alkyl moieties can be related to their lability, providing (or not) a vacant site on the coordination sphere of the metal, which, in turn, significantly impacts the reactivity of the complex. Consequently, the study of the dynamics of such species has been the focus of much attention from both experimental[14] and theoretical approaches,[15] most of them related to the estimation of the migratory insertion barriers in the context of the polymerization of olefins.[16]

The subtle balance between geometric and electronic effects on the strength of such weak interactions is not evident for late transition metal complexes yet.[4e] Among others, some relevant factors would include electronic characteristics of the metals,[17] steric requirements such as the size of substituents on ligands,[18] *trans* influence,[19] or solvent effects.[20]

A survey of the literature revealed that rhodium complexes bearing simultaneously hydride and olefin ligands—or their isomeric alkyl-agostic structures—are quite scarce, being limited to $[Rh(C_2H_4)(H)(P^iPr_3)_2]$,[21] cyclopentadienylrhodium complexes,[22] rhodacarborane species,[23] and the more recently reported with pincer type ligands.[14b,24]

Anionic P-based tripodal ligands such as $PhBP_3^-$ ($PhBP_3^-$ = $PhB(CH_2PPh_2)_3^-$) have not been explored before in this field, while they show the additional attractive of labeling three positions in octahedral complexes (by means of the NMR active phosphorus nuclei). Consequently, the "$Rh(PhBP_3)$" scaffold seems to be particularly adequate for the study of dynamics undergone by Rh-agostic species. Additionally, $PhBP_3^-$ binds strongly to rhodium,[25] allowing the development

Received: January 18, 2016

DOI: 10.1021/acs.organomet.6b00036
Organometallics XXXX, XXX, XXX−XXX

of a rich chemistry including oxygen activation,[26] stabilization of unusual tetrahedral environments for rhodium(I),[27] multiple Rh═N bonds with imido ligands,[28] and catalysis such as the selective hydrogenation of C═C bonds in α,β-unsaturated substrates,[29] and coupling of aldehydes to esters,[30] both catalyzed by the highly reactive bis(hydride) complex [Rh(PhBP$_3$)(H)$_2$(NCMe)]. While relevant for catalysis, the easy and fast hydrogen transfer of the hydride ligands in [Rh(PhBP$_3$)(H)$_2$(NCMe)] to olefins prevents its use as reagent for the stepwise study of olefin insertion reactions. Therefore, attention was focused on the monohydride version [Rh(PhBP$_3$)(H)(NCMe)$_2$]$^+$ ([**1**]$^+$), straightforwardly prepared by protonation of one of the hydride ligands of [Rh(PhBP$_3$)(H)$_2$(NCMe)] in acetonitrile.[25a] Complex [**1**]$^+$ combines a single hydride ligand with two labile acetonitrile ligands, making it a valuable precursor for the study of olefin coordination to Rh(III) species and further insertion reactions. Herein, we report a combined experimental and theoretical study on this topic including a full picture of the fluxional behavior undergone by the β-agostic complex [Rh(PhBP$_3$)(CH$_2$CH$_2$-μ-H)(NCMe)]$^+$ ([**3**]$^+$), which in turn, sheds light on the potential dynamics of such species. In addition, the determining role of entropy and steric effects in the migratory insertion of olefins into M−H bonds is also reported.

RESULTS AND DISCUSSION

Energetics for Dissociation of Acetonitrile in Complex [Rh(PhBP$_3$)(H)(NCMe)$_2$]$^+$ ([1]$^+$). The feasibility for the dissociation of the acetonitrile in complex [Rh(PhBP$_3$)(H)(NCMe)$_2$]$^+$ ([**1**]$^+$)—to eventually produce the species [Rh(PhBP$_3$)(H)(NCMe)]$^+$ ([**2**]$^+$), Figure 1—was experimentally

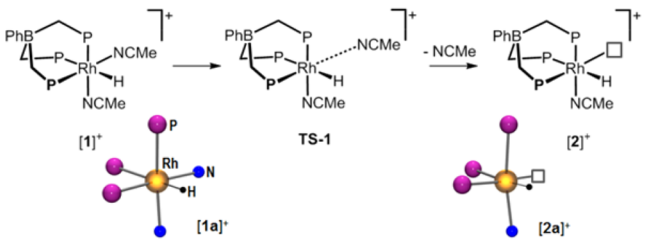

Figure 1. Acetonitrile dissociation from [**1**]$^+$ and DFT modeled structures for complexes [**1a**]$^+$ and [**2a**]$^+$. Only the P atoms of PhBP$_3^-$ (purple) and N atoms of acetonitrile (blue) are shown for clarity.

evaluated from the VT-^{1}H NMR spectra in d^8-toluene, a solvent in which [**1**]$^+$ is slightly soluble. On heating, broad-line effects on the signal corresponding to acetonitrile were clearly observable in the ^{1}H NMR spectra. Simulation of the spectra and fitting the chemical exchange rate constants (k) into the Eyring equation gave the activation parameters $\Delta H^{\ddagger}$ = 16.3 ± 1 kcal mol^{-1} and $\Delta S^{\ddagger}$ = 3 ± 2 cal mol^{-1} K^{-1} (see Supporting Information). In separate experiments, the dependence of k with the concentration of acetonitrile was examined. Values of k were found to be independent of the concentration of MeCN, indicating that they correspond to the rates of acetonitrile dissociation from [**1**]$^+$. Moreover, the low value for the activation entropy (3 ± 2 kcal mol^{-1} K^{-1}) agrees with a transition state like **TS-1**, in which the departing acetonitrile is still close to rhodium (Figure 1).

Complex [Rh(PhBP$_3$)(H)(NCMe)$_2$]$^+$ ([**1a**]$^+$) and the pentacoordinated species [Rh(PhBP$_3$)(H)(NCMe)]$^+$ ([**2a**]$^+$) have been studied by DFT methods using the full molecules as models. Stationary points for both complexes were located. The calculated structure for the hydride bis(acetonitrile) complex, [Rh(PhBP$_3$)(H)(NCMe)$_2$]$^+$ ([**1a**]$^+$), shows rhodium in an octahedral geometry while rhodium displays a square pyramid geometry in [**2a**]$^+$, as commonly observed for d^6-RhL$_5$ compounds. Two protons of the phenyl groups in [**2a**]$^+$ were found to be placed in close proximity to rhodium (3.339 and 2.907 Å) providing, probably, some stabilization to this intermediate.

Acetonitrile dissociation from [**1a**]$^+$ was analyzed by modeling the structures obtained from the separation of one NCMe ligand from rhodium up to 7 Å. However, the transition state **TS-1** (Figure 1) could not be found since a continuum of energy was obtained with no clear maximum. Nonetheless, the difference in enthalpy between [**1a**]$^+$ and [**2a**]$^+$ from DFT was found to be 17.8 kcal mol^{-1}, a value that nicely fits to that experimentally calculated ($\Delta H^{\ddagger}$ = 16.3 ± 1 kcal mol^{-1}). Therefore, extrusion of acetonitrile from [**1**]$^+$ is a feasible process expected to occur at room temperature.

Reactions of Complex [Rh(PhBP$_3$)(H)(NCMe)$_2$]$^+$ ([1]$^+$) with Ethylene. Saturation of a CD_2Cl_2 solution of [**1**]$^+$ with ethylene at −30 °C causes ethylene insertion into the Rh−H bond to produce an equilibrium with the β-agostic complex [Rh(PhBP$_3$)(CH$_2$CH$_2$-μ-H)(NCMe)]$^+$ ([**3**]$^+$) and acetonitrile (Figure 2). The reaction was found to be reversible, and

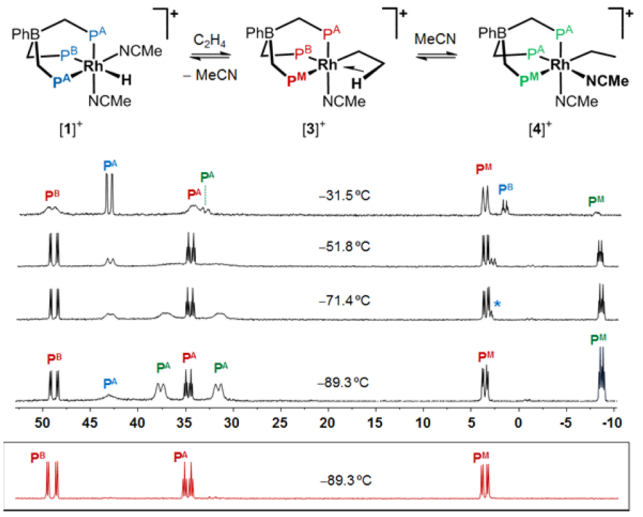

Figure 2. VT-^{31}P{^{1}H} NMR spectra of the reaction mixture of the hydride complex [Rh(PhBP$_3$)(H)(NCMe)$_2$]$^+$ ([**1**]$^+$) with ethylene in CD_2Cl_2 (in black). The ^{31}P{^{1}H} of pure samples of the β-agostic complex [**3**]$^+$ is shown in red (bottom trace) for comparative purposes.

addition of acetonitrile to the reaction mixture fully shifts the equilibrium toward [**1**]$^+$. On the contrary, no new species were observed after pressurizing the NMR tube with ethylene (3 bar). Moreover, no experimental evidence for the hydride ethylene complex [Rh(PhBP$_3$)(C$_2$H$_4$)(H)(NCMe)]$^+$ was found even carrying out the reaction at −90 °C. On the contrary, the related ethylbis(acetonitrile) complex [Rh(PhBP$_3$)(CH$_2$CH$_3$)(NCMe)$_2$]$^+$ ([**4**]$^+$) was clearly detected in the low temperature region (Figure 2).

The slow rotation of the phenyl groups on the PhBP$_3^-$ ligand in [**4**]$^+$ at −90 °C breaks the symmetry plane that relates the two halves of the molecule, so that two resonances were observed for the phosphorus nuclei *trans* to the acetonitrile

DOI: 10.1021/acs.organomet.6b00036
Organometallics XXXX, XXX, XXX−XXX

ligands (P^A). In fact the very likely, regular propeller-like orientation of the Ph groups results in a chiral structure where the P^A atoms are diastereotopic. A similar effect, although less pronounced, was observed for complex $[1]^+$ (Figure 2). However, signals corresponding to the phosphorus nuclei *trans* to the hydrido and ethyl ligands (P^B and P^M, respectively) remained almost unaltered. They were found to be high field shifted, as generally observed for phosphorus placed *trans* to ligands with a strong *trans* influence.[31] The rest of the resonances for complex $[4]^+$ agree with the proposed structure (see Supporting Information).

According to its formula, the agostic complex $[Rh(PhBP_3)(CH_2CH_2\text{-}\mu\text{-}H)(NCMe)]^+$ ($[3]^+$, Figure 2) should be the major species at low acetonitrile concentration. Moreover, it is the product from the direct protonation of the rhodium(I) complex $[Rh(PhBP_3)(CH_2{=}CH_2)(NCMe)]$ (**5**). At this point, it should be indicated that repeated preparations of **5** lead to orange crystalline solids of composition **5**·2NCMe.[25a] Therefore, further treatment of these solids with HBF_4 produces similar equilibria to those obtained from the reaction of $[1]^+$ with ethylene commented above.

Complex **5** is quite unstable in solution but stable enough for a fast recrystallization by solution in toluene and precipitation with hexane. This methodology produces a yellow solid, poorly soluble in toluene, which contains less than 1 mol % (per mol of **5**) of acetonitrile of crystallization (^{1}H NMR evidence). Reaction of these solids with HBF_4 in dichloromethane gave $[Rh(PhBP_3)(CH_2CH_2\text{-}\mu\text{-}H)(NCMe)]^+$ ($[3]^+$) in almost quantitative yield (Figure 2, red trace). The reaction was found to be instantaneous, as indicated by a color change from yellow to pale yellow. Attempts to isolate $[3]^+$ as a solid systematically produced mixtures of unidentified complexes and therefore it was characterized "in situ". Thus, three well-defined resonances were observed in the $^{31}P\{^1H\}$ NMR spectrum at −89.3 °C, (Figure 2, red trace), while the ethyl group produces three signals in a 1:1:3 ratio in the ^{1}H NMR spectrum that correspond to the two diastereotopic methylene protons and the methyl group, respectively (see Supporting Information).

Equilibria between Complexes $[1]^+$, $[3]^+$, and $[4]^+$. Detection of the equilibria between the title complexes was achieved by VT-^{1}H selective NOE NMR spectra (selnOe); two of them are shown in Figure 3. The equilibrium between $[3]^+$ and $[4]^+$ is clearly evidenced in the selnOe spectrum at −21.6 °C upon irradiation of the methyl group of the *β*-agostic

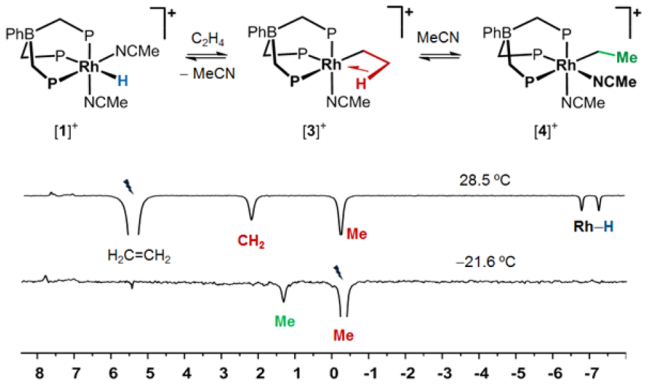

Figure 3. Selective NOE (selnOe) spectra upon irradiation of selected resonances (indicated with a ray) of the reaction mixture from the hydride complex $[Rh(PhBP_3)(H)(NCMe)_2]^+$ ($[1]^+$) and ethylene in CD_2Cl_2.

species, which produces an exchange peak with the methyl group in the ethyl complex $[4]^+$. No exchange signal was observed for the hydride resonance of $[1]^+$, suggesting that equilibrium involving $[1]^+$ is a higher energy process.

At 28.5 °C, the participation of $[1]^+$ is clearly detected from the exchange peaks observed upon irradiation of the signal corresponding to free ethylene. Notice that the two methylenic protons of the *β*-agostic complex (H^{2a} and H^{2b}) are chemically equivalent at this temperature. These NMR short-time-consuming experiments allow the different dynamic processes observed by ^{1}H NMR to be organized in a qualitative, but precise, way.

The van't Hoff plot, obtained from the integral data of the VT- ^{1}H NMR spectra, gave the thermodynamic parameters listed in Table 1 (see Supporting Information for details). In

Table 1. Experimental Thermodynamic Data[a] for Reactions Involving Complexes $[1]^+$, $[3]^+$, and $[4]^+$

reaction	$[3]^+ + NCMe \leftrightarrows [1]^+ + C_2H_4$ (1)	$[3]^+ + NCMe \leftrightarrows [4]^+$ (2)
$\Delta H°$	−2.6 ± 0.4	−6.3 ± 0.2
$\Delta S°$	−5 ± 1	−23 ± 1
$\Delta G°_{298.15}$	−1.1	0.4
$\Delta G°_{198.15}$	−1.61	−1.86
T range	−30 to 30 °C	−90 to −30 °C

[a] $\Delta H°$ and $\Delta G°$ in kcal mol^{-1}, $\Delta S°$ in cal mol^{-1} K^{-1}.

both reactions, a negative value of enthalpy was found, which indicates that both reactions are exothermic, with the ethyl complex $[4]^+$ and the hydride compound $[1]^+$ being lower in enthalpy than the *β*-agostic species $[3]^+$.

However, the entropy change is also negative in both cases. For equilibrium 2, the value of −23 ± 1 cal mol K^{-1} mainly corresponds to coordination of acetonitrile to rhodium, while for the first one, the smaller value of −5 ± 1 cal mol K^{-1} mainly reflects the difference between acetonitrile versus ethylene (as an ethyl group) coordination. Looking at the reactions in the opposite sense, formation of the *β*-agostic complex $[3]^+$ is endothermic, but in both cases, the entropy change is positive. Therefore, the formation of the *β*-agostic complex $[3]^+$ from $[1]^+$ or $[4]^+$ is an entropy-driven reaction, in which acetonitrile dissociation from both the ethyl and the hydride complexes is the driving force.

Data in Table 1 also account for the experimental observation that the addition of acetonitrile to the *β*-agostic complex quantitatively produces the hydride complex $[1]^+$ rather than the expected ethyl complex $[4]^+$. Indeed, a value of $\Delta G°_{298.15}$ of −1.5 kcal mol^{-1} can be estimated for the reaction $[4]^+ \leftrightarrows [1]^+ + C_2H_4$ from data in Table 1.

DFT Studies on the *β*-Agostic Complex $[3a]^+$ and the Related Ethyl Rotamers $[3b]^+$ and $[3c]^+$. Complex $[3]^+$ was first examined by a DFT study (b3-lyp, LanL2DZ, and 6-31G**) using the full complex $[Rh\{PhB(CH_2PPh_2)_3\}(C_2H_4\text{-}\mu\text{-}H)(NCMe)]$ ($[3a]^+$) as a model. The BF_4^- counteranion was not included, since evidence for its noncoordination to rhodium was obtained from dosy experiments. Thus, a value for the diffusion coefficient of 19.04 m^2 s^{-1} corresponding to a hydrodynamic radius of 2.89 Å was obtained from ^{19}F-dosy NMR spectra of $[3]BF_4$ in CD_2Cl_2. These values correspond well with that reported for the BF_4^- anion in inorganic salts such as $LiBF_4$.[32]

An energy minimum was found for the *β*-agostic complex $[3a]^+$ with a Rh···H[3a] distance of 2.278 Å, which lies in the

DOI: 10.1021/acs.organomet.6b00036
Organometallics XXXX, XXX, XXX−XXX

observed range (1.69−2.52 Å) for Rh···HC interactions.[6c,10,12f,23b,33] Nonetheless, a more precise structure was obtained with LanL2TZ(f), which uses the f-polarization functions developed by Frenking's group,[34] allowing a better representation of the secondary interactions. With this basis set, the Rh···H^{3a} distance reduces to 2.083 Å, a value that matches much better with that expected. Therefore, all the rest of the intermediates and transition states described below (as well as the above commented complexes [**1a**]$^+$ and [**2a**]$^+$) have been calculated at the same level of theory for comparative purposes.

The β-agostic interaction in [**3a**]$^+$ is also associated with an elongation of the corresponding C$^\beta$−H^{3a} bond distance (1.143 Å) if compared with the other two C$^\beta$−H$^{3b/3c}$ bond distances (Figure 4, left). The carbon−carbon distance in the ethyl group

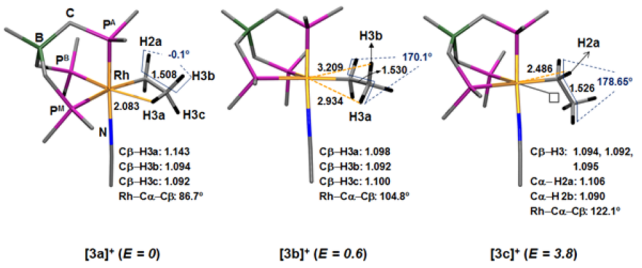

Figure 4. DFT calculated structures for complexes [**3a**]$^+$, [**3b**]$^+$, and [**3c**]$^+$. Values of energy are given in kcal mol^{-1} and C−H bond distances in Å. Only C^{ipso} of the phenyl groups and protons of the ethyl group are shown for clarity.

elongates from 1.443(7) Å observed in [Rh(PhBP$_3$)(CH$_2$=CH$_2$)(NCMe)] (**5**) to 1.508 Å according to the presence of a single C−C bond. Moreover, the coordination polyhedron of the metal is close to the octahedron with C$^\alpha$ *trans* to P^M, N *trans* to P^A, and the methyl group approaching to the position *trans* to P^B. Furthermore, the eclipsed conformation of the ethyl group also supports the β-agostic interaction, since otherwise a staggered conformation should be expected.

Two related minima close in energy, [**3b**]$^+$ and [**3c**]$^+$, were also found, and their structures are shown in Figure 4. Both isomers are better described as nonagostic ethyl complexes, which is remarkable since such type of isomers have been considered high energy species.[14b,15b,f] [**3b**]$^+$ and [**3c**]$^+$ show a staggered conformation for the ethyl group in contrast to the eclipsed conformation found for [**3a**]$^+$ (Figure 4).

In addition, isomer [**3b**]$^+$ shows very long Rh···H$^{3a/3b}$ distances while the C$^\beta$−H$^{3a/3b/3c}$ bond distances are almost identical. Concerning isomer [**3c**]$^+$, it could be considered as an α-agostic species, but the H^{2a} proton is far away from the coordination vacancy—represented with a square in Figure 4 (right)—leading to a quite long Rh···H^{2a} distance. A major difference between the ethyl complexes [**3b**]$^+$ and [**3c**]$^+$ comes from the orientation of the ethyl group in such a way that the methyl group is placed in the region corresponding to the sixth position of the octahedron in [**3b**]$^+$, while it is fully eclipsed to the acetonitrile ligand in [**3c**]$^+$. This orientation is associated with an opening of the angle Rh−C$^\alpha$−C$^\beta$, in [**3c**]$^+$ relative to [**3b**]$^+$, and, most probably, it is the origin of the higher energy found for [**3c**]$^+$.[35]

A comparison between isomers [**3a**]$^+$ and [**3b**]$^+$ indicates that the small difference in energy between them represents the balance of cleaving the agostic interaction versus the stabilization provided by the conformational change of the ethyl group from eclipsed to staggered. Since this difference for ethane is about 2.8 kcal mol^{-1}, the β-agostic interaction in [**3a**]$^+$ can be estimated as ca. 2.8 + 0.6 = 3.5 kcal mol^{-1}.[36]

The three isomers easily interconvert through transition states **TS-2** and **TS-3** (Figure 5). The gray path relates [**3a**]$^+$

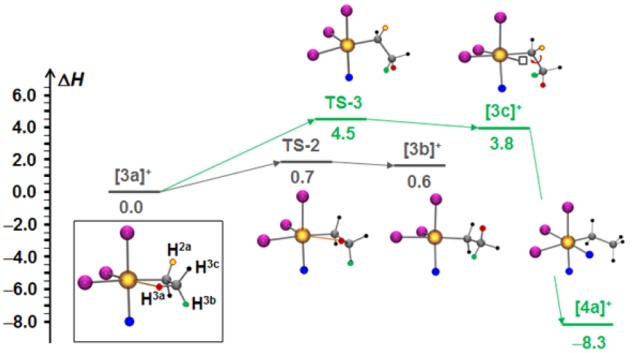

Figure 5. Energy profile for transformations between [**3a**]$^+$, [**3b**]$^+$, [**3c**]$^+$, and the ethyl bis(acetonitrile) complex [**4a**]$^+$. Values of ΔH are given in kcal mol^{-1}. Only the P atoms of PhBP$_3^-$ (purple) and N atoms of acetonitrile (blue) are shown for clarity.

with [**3b**]$^+$, and corresponds to the "in place rotation", responsible for the chemical equivalence of the methylenic protons H^{3a}, H^{3b}, and H^{3c}. The process has practically no energy barrier, and accordingly, the three methyl protons are chemically equivalent in the ^{1}H NMR spectrum of [**3**]$^+$ at −90 °C.

The path in green connects [**3a**]$^+$ to [**3c**]$^+$ and then to the ethyl bis(acetonitrile) complex [**4a**]$^+$ after acetonitrile coordination to the vacant site in [**3c**]$^+$. The enthalpy value for the reaction [**3a**]$^+$ + NCMe ⇆ [**4a**]$^+$ has been estimated as −8.3 kcal mol^{-1}, in good agreement with the experimental value of −6.3 kcal mol^{-1} measured experimentally (Table 1).

Energy Profile for Equilibrium between Complexes [1a]$^+$ and [3a]$^+$. The reaction of the hydride [Rh(PhBP$_3$)(H)(NCMe)$_2$]$^+$ ([**1**]$^+$) with ethylene leading to [Rh(PhBP$_3$)(CH$_2$CH$_2$-μ-H)(NCMe)]$^+$ ([**3**]$^+$) would require the three elementary steps depicted in Figure 6: (i) acetonitrile dissociation, (ii) ethylene coordination, and (iii) ethylene insertion into the Rh−H bond. The first step gives the square-pyramidal complex [Rh(PhBP$_3$)(H)(NCMe)]$^+$ ([**2a**]$^+$) as commented above. Ethylene coordination renders the hydride ethylene complex [Rh(PhBP$_3$)(C$_2$H$_4$)(H)(NCMe)]$^+$ ([**6a**]$^+$) and takes place through a transition state **TS-4** whose enthalpy is similar to that of the intermediate [**2a**]$^+$. Ethylene insertion in [**3a**]$^+$ occurs with a low energy barrier (2.5 kcal mol^{-1}) through the transition state **TS-5**, which was also found to possess an agostic interaction (see Supporting Information).

From a thermodynamic point of view, the calculated enthalpy for the equilibrium [**3a**]$^+$ + NCMe ⇆ [**1a**]$^+$ + C$_2$H$_4$ was estimated as −4.7 kcal mol^{-1}, in good agreement with that experimentally measured (−2.6 kcal mol^{-1}, Table 1).

Under a kinetic perspective, the activation barrier for the transformation of the hydride complex [**1a**]$^+$ into the β-agostic species [**3a**]$^+$ is mainly determined by the acetonitrile extrusion ($\Delta H^‡$ = 16.3 ± 1.0 kcal mol^{-1} by NMR and ca. 17.8 kcal mol^{-1} by DFT) or the ethylene coordination through **TS-4** ($\Delta H^‡$ = 18.3 by DFT), which prevents direct measurements of the barrier for the ethylene insertion by NMR.

DOI: 10.1021/acs.organomet.6b00036
Organometallics XXXX, XXX, XXX−XXX

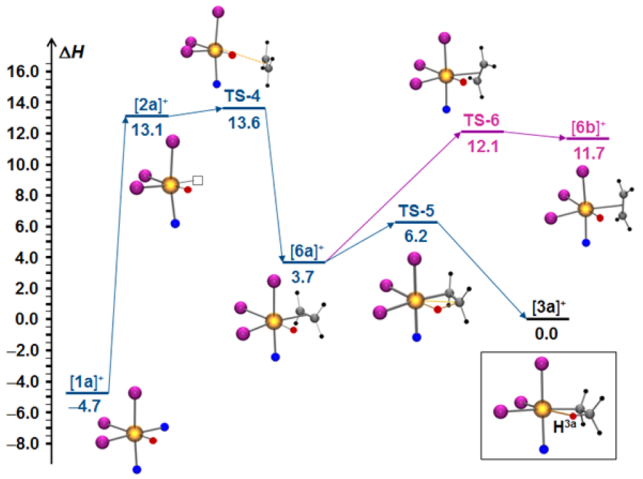

Figure 6. Energy profile for the reaction of $[Rh(PhBP_3)(H)(NCMe)_2]^+$ ($[\mathbf{1a}]^+$) with ethylene to give the β-agostic complex $[Rh(PhBP_3)(CH_2CH_2\text{-}\mu\text{-}H)(NCMe)]^+$ ($[\mathbf{3a}]^+$). Values of ΔH are given in kcal mol^{-1}. Only the P atoms (purple) of $PhBP_3^-$ and N atoms (blue) of acetonitrile are shown for clarity.

Figure 6 also includes the isomer of the hydrido−ethylene complex $[\mathbf{6b}]^+$, in which the ethylene ligand is rotated 90° and lies higher in enthalpy by 8.0 kcal mol^{-1} relative to $[\mathbf{6a}]^+$.

Ethylene rotation (path in purple) takes place through the accessible transition state **TS-6** in which ethylene is twisted in around 23°.

Fluxional Behavior of Complex $[\mathbf{3}]^+$ in Solution. The dynamic processes undergone by the β-agostic complex $[\mathbf{3}]^+$ were examined by VT-$^{31}P\{^1H\}$ NMR. Experimental line shapes were compared to calculated ones by using the gNMR simulation program,[37] and a set of observed and simulated spectra is shown in Figure 7. Two different rate constants were required to reproduce the experimental spectra. The first one (k_{P1}) corresponds to the process that equilibrates P^A with P^B, while the second one (k_{P2}) is responsible of the equilibration of P^A/P^B with P^M.

Fitting the data into the corresponding Eyring plots gives the activation parameters: $\Delta H_1^{\ddagger}$ = 11.4 ± 0.4 kcal mol^{-1}, $\Delta S_1^{\ddagger}$ = −0 ± 1 cal mol^{-1} K^{-1} for the first one and $\Delta H_2^{\ddagger}$ = 12.8 ± 0.5 kcal mol^{-1}, $\Delta S_2^{\ddagger}$ = −0.5 ± 1 cal mol^{-1} K^{-1} for the second one (see Supporting Information for details).

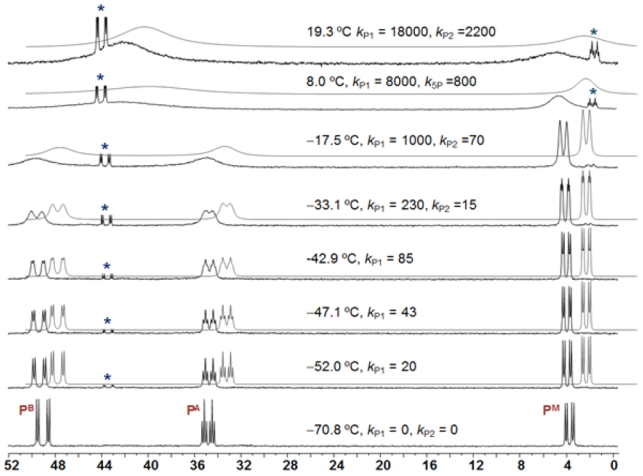

Figure 7. Experimental and calculated (traces in gray) VT-$^{31}P\{^1H\}$ NMR spectra of $[Rh(PhBP_3)(CH_2CH_2\text{-}\mu\text{-}H)(NCMe)]^+$ ($[\mathbf{3}]^+$) in CD_2Cl_2. The asterisk denotes signals corresponding to the hydride complex $[\mathbf{1}]^+$.

The simplest explanation for both fluxional processes is illustrated in Scheme 1. Starting from isomer $[\mathbf{3c}]^+$, a shift of

Scheme 1. Dynamic Processes Undergone by Complex $[\mathbf{3}]^+$ in Solution Detected by $^{31}P\{^1H\}$ NMR

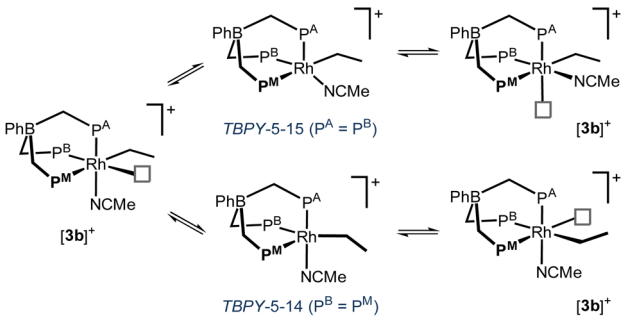

acetonitrile to the coordination vacancy equilibrates P^A with P^B, while moving the ethyl group to the coordination vacancy equilibrates P^B with P^M. Both processes would take place through the corresponding *TBPY* geometries, so that the small difference in the enthalpy measured experimentally would represent the difference between the geometries *TBPY*-5-15 and *TBPY*-5-14.

Attempts to find these *TBPY* geometries as transition states by DFT failed, but it was possible to find the related *TBPY*-5-14 starting from the simplest species containing a hydride ligand instead of the ethyl group $[Rh(PhBP_3)(H)(NCMe)]^+$ ($[\mathbf{2a}]^+$) (see Supporting Information). Thus, the difference in enthalpy between SPY-$[\mathbf{2a}]^+$ and *TBPY*-5-14-$[\mathbf{2a}]^+$ was found to be 11.0 kcal mol^{-1}, which lies in the range of the measured values for the acetonitrile shift or ethyl shift in the β-agostic complex $[\mathbf{3}]^+$. Notice that any process shown in Scheme 1 also equilibrates H^{2a}/H^{2b} (the methylenic protons of the ethyl group), for which the energy barrier has been rarely measured experimentally.

An intriguing feature of the VT-$^{31}P\{^1H\}$ spectra (Figure 7) is the "appearance" of the hydride complex $[\mathbf{1}]^+$, whose signals increase in intensity on raising temperature, and certainly, this is not a problem of solubility of $[\mathbf{1}]^+$ in CD_2Cl_2. Therefore, the most reasonable proposal to explain this observation is to consider the existence of an additional source of acetonitrile in solution. Consequently, dissociation of acetonitrile from both the β-agostic species and the hydride olefin intermediate $[Rh(PhBP_3)(H)(C_2H_4)(NCMe)]^+$ ($[\mathbf{6a}]^+$) have also been analyzed by DFT studies.

DFT Studies on the β-Agostic $[Rh(PhBP_3)(CH_2CH_2\text{-}\mu\text{-}H)]^+$ ($[\mathbf{8a}]^+$) and Related Complexes. Figure 8 shows the energy profile corresponding to the extrusion of acetonitrile from $[\mathbf{6a}]^+$ and $[\mathbf{3a}]^+$; both processes converge into the β-agostic species $[Rh(PhBP_3)(CH_2CH_2\text{-}\mu\text{-}H)]^+$ ($[\mathbf{8a}]^+$). Starting from $[\mathbf{6a}]^+$, the dissociation of acetonitrile produces the square-pyramidal complex $[Rh(PhBP_3)(H)(C_2H_4)]^+$ ($[\mathbf{7a}]^+$), and the insertion of ethylene into the Rh−H bond to give $[Rh(PhBP_3)(CH_2CH_2\text{-}\mu\text{-}H)]^+$ ($[\mathbf{8a}]^+$) occurs through the transition state **TS-7**. Nonetheless, the direct dissociation of acetonitrile from $[Rh(PhBP_3)(CH_2CH_2\text{-}\mu\text{-}H)(NCMe)]^+$ ($[\mathbf{3a}]^+$) produces an alternative path lower in enthalpy.

Complex $[Rh(PhBP_3)(CH_2CH_2\text{-}\mu\text{-}H)]^+$ ($[\mathbf{8a}]^+$) was found to be 16.6 kcal mol^{-1} (in enthalpy) higher than $[Rh(PhBP_3)$-

DOI: 10.1021/acs.organomet.6b00036
Organometallics XXXX, XXX, XXX−XXX

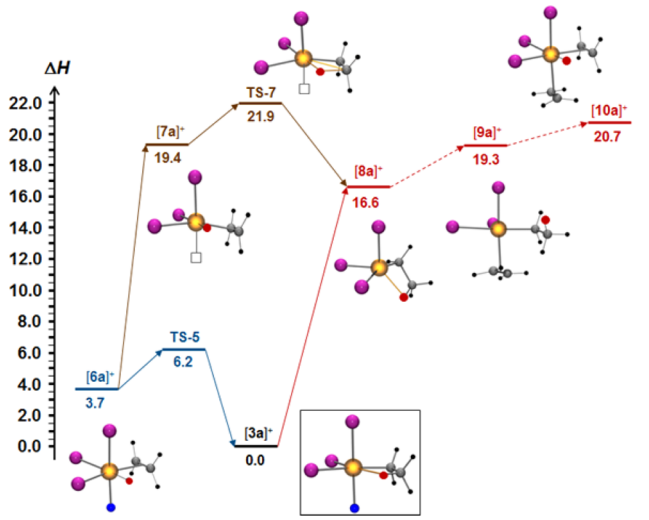

Figure 8. Energy profile for the extrusion of acetonitrile from $[\mathbf{6a}]^+$ and $[\mathbf{3a}]^+$. Values of ΔH are given in kcal mol^{-1}. Only the P atoms (purple) of $PhBP_3^-$ and N atoms (blue) of acetonitrile are shown for clarity.

$(CH_2CH_2\text{-}\mu\text{-}H)(NCMe)]^+$ ($[\mathbf{3a}]^+$), a value slightly smaller than that found for the extrusion of acetonitrile from the hydride complex $[Rh(PhBP_3)(H)(NCMe)_2]^+$ ($[\mathbf{1a}]^+$) to give $[Rh(PhBP_3)(H)(NCMe)]^+$ ($[\mathbf{2a}]^+$, 17.8 kcal mol^{-1}). Since the entropy change associated with the dissociation of acetonitrile is expected to be similar for both reactions (from $[\mathbf{1a}]^+$ and from $[\mathbf{3a}]^+$), we can conclude than complex $[\mathbf{8a}]^+$ is indeed present in solution. Moreover, the formation of $[\mathbf{8a}]^+$ is the origin of the additional source of acetonitrile in the reaction medium.

Agostic complexes with low electron counts are very unusual, although complexes $[Rh(POCOP)(CH_2CH_2\text{-}\mu\text{-}H)]^+$ (POCOP = 2,6-bis(di-*tert*-butylphosphinito)benzene),[14b] $[Rh(C_5Me_5)(CH_2CH_2\text{-}\mu\text{-}H)]^+$,[15c] and $[Rh(P^iPr_3)_2(CH_2CH_2\text{-}\mu\text{-}H)]^+$,[21] have been studied by DFT in rhodium chemistry.

From a thermodynamic point of view, a value of $\Delta G^\circ_{298} = -3.9$ kcal mol^{-1} has been calculated for the reaction shown in Scheme 2, which accounts for the experimental observations just commented.

Scheme 2. Transformation of β-Agostic Complex $[\mathbf{3a}]^+$ into Complexes $[\mathbf{8a}]^+$ and $[\mathbf{1a}]^+$

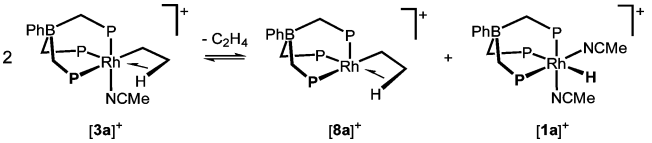

For comparative purposes, the ethyl complex $[Rh(PhBP_3)(C_2H_4)(CH_2CH_3)]^+$ ($[\mathbf{9a}]^+$) and the hydride bis(ethylene) counterpart $[Rh(PhBP_3)(C_2H_4)_2(H)]^+$ ($[\mathbf{10a}]^+$) have also been calculated at the same level of theory. For the addition of a second molecule of ethylene to $[\mathbf{8a}]^+$ (Figure 8) the enthalpy changes are small but the entropy change is strong leading thus to large and positive values for ΔG°_{298}. In good agreement, neither $[\mathbf{9a}]^+$ nor $[\mathbf{10a}]^+$ was observed in solution. Figure 9 displays selected structural parameters for complexes $[\mathbf{8a}]^+$ and $[\mathbf{9a}]^+$ enlightening their different nature. While $[\mathbf{8a}]^+$ is clearly a β-agostic compound, the related $[\mathbf{9a}]^+$

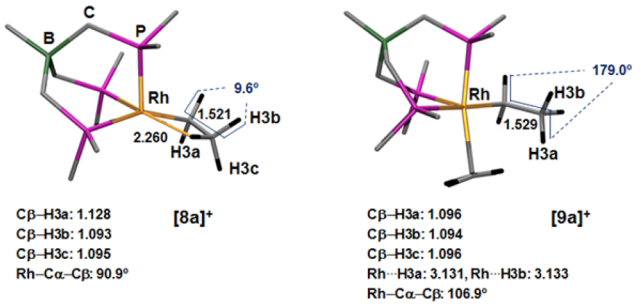

Figure 9. DFT calculated structures for complexes $[\mathbf{8a}]^+$ and $[\mathbf{9a}]^+$. Distances are given in Å. Only C^{ipso} of the phenyl groups and protons of the ethyl group are shown for clarity.

is better described as a terminal nonagostic ethyl complex according to the preceding comments for complexes $[\mathbf{3a}]^+$, $[\mathbf{3b}]^+$, and $[\mathbf{3c}]^+$ (Figure 4).

Further Comments on β-Agostic Rhodium Species. The study reported here provides a unique opportunity to analyze the subtle influence of electronic and steric factors on the strength of the β-agostic interaction and on the driving force that favors (or not) the transfer of the hydrogen to the metal. As nicely depicted in Table 2, the strength of the β-

Table 2. Selected Parameters for Complexes Shown and ΔH° for the β-Hydride Elimination Reaction to the Corresponding Hydrido–Ethylene Compound[a]

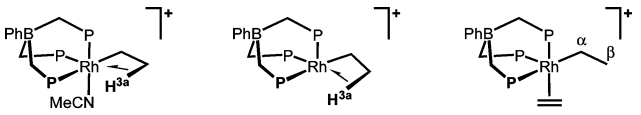

	$[\mathbf{3a}]^+$	$[\mathbf{8a}]^+$	$[\mathbf{9a}]^+$
$Rh\cdots H^{3a}$ (Å)	2.084	2.260	3.131
$Rh–C^\alpha–C^\beta$ (deg)	86.74	90.94	106.87
$H–C^\alpha–C^\beta–H$ (deg)	0.09	9.63	176.64
ΔH°	+3.7	+2.8	+1.4

[a]Values of ΔH° are given in kcal mol^{-1}.

agostic interaction, evidenced by shorter $Rh\cdots H^{3a}$ distances, more acute $Rh–C^\alpha–C^\beta$ angles, and smaller torsion angles for the protons of the ethyl groups, decreases on going from $[\mathbf{3a}]^+$ to $[\mathbf{9a}]^+$, complex $[\mathbf{9a}]^+$ being a nonagostic species, but $[\mathbf{8a}]^+$ and $[\mathbf{3a}]^+$ being clearly β-agostic compounds.

Of particular relevance is the highly unsaturated complex $[\mathbf{8a}]^+$, which lies between $[\mathbf{3a}]^+$ and $[\mathbf{9a}]^+$ (despite containing the most electrophilic rhodium center) since it is universally accepted that shorter $M\cdots H^{3a}$ bond distances (associated with stronger interactions) come from more electrophilic metal centers. Moreover, addition of a ligand to $[\mathbf{8a}]^+$ can either fully destroy the β-agostic interaction or reinforce it, as exemplified by complexes $[\mathbf{9a}]^+$ and $[\mathbf{3a}]^+$, respectively. In any case, the beneficial role of the acetonitrile ligand on the stabilization of the β-agostic interaction is remarkable

Values of enthalpy relative to their corresponding hydrido–ethylene counterparts follow a similar trend in such a way that the three ethyl complexes in Table 2 are more stable than the corresponding hydride–ethylene counterparts. This constitutes a quite unusual situation in rhodium chemistry,[38] since the general trend is just the opposite (as expected for second row transition metals). Since other factors such as *trans* or solvent

DOI: 10.1021/acs.organomet.6b00036
Organometallics XXXX, XXX, XXX–XXX

effects can be excluded, the steric pressure exerted by the phenyl groups on the $PhBP_3^-$ ligand should be the key factor that favors the inserted products versus the hydrido−ethylene derivatives, since the former are expected to be less constrained structures than the latter.

A third aspect considered concerns the energy barriers for two closely related processes: the "in place rotation" (E^i) and the β-hydride elimination reaction (E^β). As schematically depicted in Scheme 3, the "in place rotation" requires the

Scheme 3. Schematic Representation of the Transition States for the Processes[a]

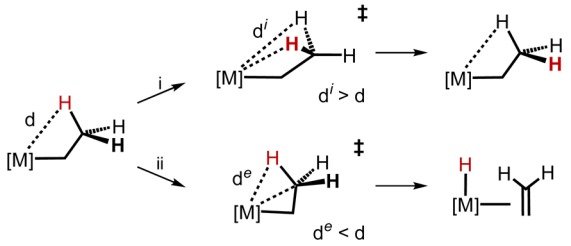

[a](i) "In place rotation" and (ii) β-hydride elimination.

cleavage of the β-agostic interaction through a transition state in which the M···H distance elongates ($d^i > d$). On the contrary, the transition state for the β-hydride elimination is associated with a shortening of such distance ($d^e < d$). It can thus be expected that stronger β-agostic interactions would require higher energy barriers for the "in place rotation", but lower ones for the β-hydrido elimination reaction. Indeed, the stronger a β-agostic interaction is, the closer the structure is to the corresponding transition state for the β-elimination. Accordingly, the data available from DFT calculations for the rhodium complexes fit nicely under this perspective (see Table 3).

Finally, other olefins such as styrene also insert into the Rh−H bond of complex $[1]^+$, although the expected complex $[Rh(PhBP_3)(CHPhCH_2\text{-}\mu\text{-}H)(NCMe)]^+$ ($[11]^+$) could not be observed by NMR. Nonetheless, it was detected by exchange spectroscopy experiments. Thus, irradiation of the hydride signal of complex $[Rh(PhBP_3)(H)(NCMe)_2]^+$ ($[1]^+$) in the presence of styrene revealed the exchange with the signals corresponding to the olefinic protons of styrene (Figure 10, right).

Structural parameters calculated by DFT for $[11a]^+$ fit well with those expected for a β-agostic complex (Figure 10, left), in which the electron withdrawing character of the phenyl group is

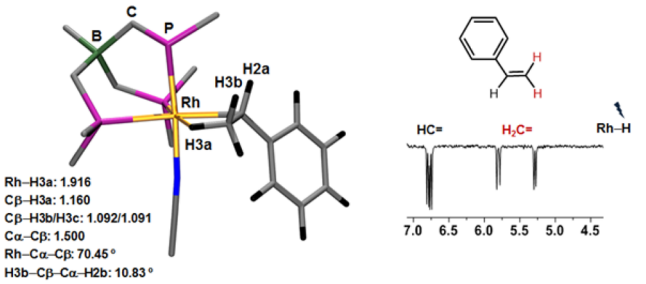

Figure 10. DFT-calculated structure for $[11a]^+$ along with selected structural parameters (left) and ^1H selnOe NMR spectrum of a solution of $[1]^+$ in the presence of 10 molar equiv of styrene upon irradiation of the signal corresponding to the hydrido ligand in $[1]^+$ (right).

reflected in a slightly short Rh···H^{3a} distance of 1.916 Å when compared to that observed in the ethyl analogue $[3a]^+$. Accordingly, the energy barrier for the "in place rotation" takes place through a transition state similar to complex $[3b]^+$ and it is associated with a $\Delta G^{\ddagger}_{298}$ value of 1.8 kcal mol^{-1} (see Supporting Information), indicating that interaction of the proton with rhodium is slightly stronger than that observed in the ethyl derivative $[3a]^+$.

SUMMARY AND CONCLUSIONS

In this paper, we have combined NMR spectroscopy and computational (DFT) studies to gain information about the stability, dynamics, and behavior in solution of β-agostic/ethyl species in complexes bearing the tripodal ligand $PhBP_3^-$. Two of them, $[Rh(PhBP_3)(CH_2CH_2\text{-}\mu\text{-}H)(NCMe)]^+$ ($[3a]^+$) and the highly unsaturated species $[Rh(PhBP_3)(CH_2CH_2\text{-}\mu\text{-}H)]^+$ ($[8a]^+$), were found to be real β-agostic complexes, while the related rotamers, $[3b]^+$ and $[3c]^+$, as well as $[Rh(PhBP_3)(C_2H_4)(CH_2CH_3)]^+$ ($[9a]^+$) are better described as nonagostic ethyl complexes. This result is remarkable, since such type of compounds have been considered as high energy species. Moreover, a comparison of complexes $[3a]^+$ and $[9a]^+$ revealed the key role of the fifth ligand in stabilizing (acetonitrile) or destroying (ethylene) the β-agostic interaction in these ethyl derivatives. Furthermore, starting from $[Rh(PhBP_3)(CH_2CH_3)(NCMe)_2]^+$ ($[4a]^+$), dissociation of acetonitrile was found to be the driving force to $[Rh(PhBP_3)(CH_2CH_2\text{-}\mu\text{-}H)(NCMe)]^+$ ($[3a]^+$); a similar behavior was observed for $[3a]^+$, which transforms into $[Rh(PhBP_3)(CH_2CH_2\text{-}\mu\text{-}H)]^+$ ($[8a]^+$) at higher temperature. Accordingly, NMR-measured

Table 3. DFT-Calculated Rh−H and Rh···H^{3a} Bond Distances (Å) in Complexes $[Rh(L_3)(L)(H)(H_2C{=}CH_2)]^+$ and $[Rh(L_3)(L)(CH_2CH_3)]^+$, Respectively, and $\Delta G^{\ddagger}_{298}$ for the Processes "In Place Rotation" (E^i) and β-Elimination Reactions (E^β) (kcal mol^{-1})

L_3	L	Rh···H^{3a}	TS[a]	Rh−H	E^i	E^β	ref
C_5H_5	$P(OMe)_3$	1.771	1.624	1.567	10.7	0	15b
C_5H_5	PMe_3	1.773	1.628	1.564	9.5	0	15b
C_5H_5	C_2H_4	1.790	1.594	1.562			15c
C_5Me_5	$P(OMe)_3$	1.818	1.629	1.466	6.7	1.6	15b
C_5Me_5	PMe_3	1.823	1.632	1.573	6.0	0.2	15b
C_5Me_5	C_2H_4	1.827	1.599	1.568			15c
$PhBP_3$	NCMe	2.083	1.621	1.561	0.44	7.35	b
$PhBP_3$		2.260	1.632	1.572	0	6.55	b

[a]Rh···H distance in the transition state connecting both species. [b]This work.

DOI: 10.1021/acs.organomet.6b00036
Organometallics XXXX, XXX, XXX−XXX

equilibrium constants for both equilibria indicate that they are entropy-driven reactions.

Notably, the three related hydride complexes $[Rh(PhBP_3)(C_2H_4)(H)(NCMe)]^+$ ($[\mathbf{6a}]^+$), $[Rh(PhBP_3)(C_2H_4)(H)]^+$ ($[\mathbf{7a}]^+$), and $[Rh(PhBP_3)(C_2H_4)_2(H)]^+$ ($[\mathbf{10a}]^+$) were found to be higher in enthalpy than the corresponding β-agostic/ethyl species. This noteworthy result for rhodium chemistry is well explained when taking into account the steric pressure exerted by the bulkier $PhBP_3^-$ ligand in comparison to other systems that have been studied. As noted earlier, small variations of electronic and steric factors can control the strength of the β-agostic interaction and will therefore determine the stability of the insertion products relative to the hydrido−ethylene species. Moreover, the stronger this interaction is, the more easily the transformation into the rhodium hydride olefin counterpart occurs. Finally, other olefins such as styrene also insert into the Rh−H bond of complex $[\mathbf{1}]^+$, as deduced from exsy experiments and DFT calculations. We believe that these findings could help in the development of new complexes suitable for C−H bond functionalization and related reactions.

■ ASSOCIATED CONTENT

Supporting Information

The Supporting Information is available free of charge on the ACS Publications website at DOI: 10.1021/acs.organomet.6b00036.

Experimental details (PDF)

X,Y,Z coordinates for DFT-calculated intermediates and transition states (XYZ)

■ AUTHOR INFORMATION

Corresponding Author

*E-mail: ctejel@unizar.es.

Present Address

†A.M.G.: School of Chemistry, University of Nottingham University Park, Nottingham, NG7 2RD, U.K.

Notes

The authors declare no competing financial interest.

■ ACKNOWLEDGMENTS

The generous financial support from MICINN/FEDER (Project CTQ2011-22516), MINECO/FEDER (Project CTQ2014-53033-P), and Gobierno de Aragón/FSE (GA/FSE, Inorganic Molecular Architecture Group, E70) is gratefully acknowledged. A.M.G. thanks GA/FSE for a fellowship. This article is dedicated to the memory of Prof. Roberto A. Sánchez-Delgado, a pioneer in chemistry, a brave fighter and an excellent friend that encouraged to one of us (C.T.) to overcome our common illness.

■ REFERENCES

(1) Selected papers and reviews: (a) Masarwa, A.; Weber, M.; Sarpong, R. *J. Am. Chem. Soc.* **2015**, *137*, 6327−6334. (b) Topczewski, J. J.; Sanford, M. S. *Chem. Sci.* **2015**, *6*, 70−76. (c) Ebe, Y.; Nishimura, T. *J. Am. Chem. Soc.* **2015**, *137*, 5899−5902. (d) Dateer, R. B.; Chang, S. *J. Am. Chem. Soc.* **2015**, *137*, 4908−4911. (e) Gandeepan, P.; Cheng, C.-H. *Chem. - Asian J.* **2015**, *10*, 824−838. (f) Yang, L.; Huang, H. *Chem. Rev.* **2015**, *115*, 3468−3517. (g) Wang, Z.; Kuninobu, Y.; Kanai, M. *J. Am. Chem. Soc.* **2015**, *137*, 6140−6143. (h) Ackermann, L. *Acc. Chem. Res.* **2014**, *47*, 281−295. (i) Tsurugi, H.; Yamamoto, K.; Nagae, H.; Kaneko, H.; Mashima, K. *Dalton Trans.* **2014**, *43*, 2331−2343. (j) Campos, J.; Kundu, S.; Pahls, D. R.; Brookhart, M.; Carmona, E.; Cundari, T. R. *J. Am. Chem. Soc.* **2013**, *135*, 1217−1220. (k) Poverenov, E.; Milstein, D. *Top. Organomet. Chem.* **2013**, *40*, 21−48. (l) Lee, S. H.; Gorelsky, S. I.; Nikonov, G. I. *Organometallics* **2013**, *32*, 6599−6604. (m) Engle, K. M.; Mei, T.-S.; Wasa, M.; Yu, J.-Q. *Acc. Chem. Res.* **2012**, *45*, 788−802. (n) Gunanathan, C.; Milstein, D. *Acc. Chem. Res.* **2011**, *44*, 588−602. (o) Cho, S. H.; Kim, J. Y.; Kwak, J.; Chang, S. *Chem. Soc. Rev.* **2011**, *40*, 5068−5083. (p) Wencel-Delord, J.; Dröge, T.; Liu, F.; Glorius, F. *Chem. Soc. Rev.* **2011**, *40*, 4740−4761. (q) Ackermann, L. *Chem. Rev.* **2011**, *111*, 1315−1345. (r) Colby, D. A.; Bergman, R. G.; Ellman, J. A. *Chem. Rev.* **2010**, *110*, 624−655. (s) Perutz, R. N.; Sabo-Etienne, S. *Angew. Chem., Int. Ed.* **2007**, *46*, 2578−2592. (t) Clot, E.; Eisenstein, O.; Jones, W. D. *Proc. Natl. Acad. Sci. U. S. A.* **2007**, *104*, 6939−6944. (u) Chen, G. S.; Labinger, J. A.; Bercaw, J. E. *Proc. Natl. Acad. Sci. U. S. A.* **2007**, *104*, 6915−6920. (v) Bernskoetter, W. H.; Schauer, C. K.; Goldberg, K. I.; Brookhart, M. *Science* **2009**, *326*, 553−556. (w) Crabtree, R. H. *J. Organomet. Chem.* **2004**, *689*, 4083−4091. (x) Hall, C.; Perutz, R. N. *Chem. Rev.* **1996**, *96*, 3125−3146.

(2) (a) Sieffert, N.; Réocreux, R.; Lorusso, P.; Cole-Hamilton, D. J.; Bühl, M. *Chem. - Eur. J.* **2014**, *20*, 4141−4155. (b) Grellier, M.; Sabo-Etienne, S. *Chem. Commun.* **2012**, *48*, 34−42. (c) Haibach, M. C.; Kundu, S.; Brookhart, M.; Goldman, A. S. *Acc. Chem. Res.* **2012**, *45*, 947−958. (d) Choi, J.; MacArthur, A. H. R.; Brookhart, M.; Goldman, A. S. *Chem. Rev.* **2011**, *111*, 1761−1779. (e) Gruver, B. C.; Adams, J. J.; Warner, S. J.; Arulsamy, N.; Roddick, D. M. *Organometallics* **2011**, *30*, 5133−5140.

(3) Brookhart, M.; Green, M. L. H. *J. Organomet. Chem.* **1983**, *250*, 395−408.

(4) For leading references and revisions: (a) Shaw, P. A.; Phillips, J. M.; Newman, C. P.; Clarkson, G. J.; Rourke, J. P. *Chem. Commun.* **2015**, *51*, 8365−8368. (b) Schmidbaur, H.; Raubenheimer, H. G.; Dobrzańska, L. *Chem. Soc. Rev.* **2014**, *43*, 345−380. (c) Saßmannshausen, J. *Dalton Trans.* **2012**, *41*, 1919−1923. (d) Montag, M.; Efremenko, I.; Diskin-Posner, Y.; Ben-David, Y.; Martin, J. M. L.; Milstein, D. *Organometallics* **2012**, *31*, 505−512. (e) Scherer, W.; Herz, V.; Brück, A.; Hauf, C.; Reiner, F.; Altmannshofer, S.; Leusser, D.; Stalke, D. *Angew. Chem., Int. Ed.* **2011**, *50*, 2845−2849. (f) Scherer, W.; Wolstenholme, D. J.; Herz, V.; Eickerling, G.; Brück, A.; Benndorf, P.; Roesky, P. W. *Angew. Chem., Int. Ed.* **2010**, *49*, 2242−2246. (g) Lein, M. *Coord. Chem. Rev.* **2009**, *253*, 625−634. (h) Etienne, M.; McGrady, J. E.; Maseras, F. *Coord. Chem. Rev.* **2009**, *253*, 635−646. (i) Brookhart, M.; Green, M. L. H.; Parkin, G. *Proc. Natl. Acad. Sci. U. S. A.* **2007**, *104*, 6908−6914. (j) Clot, E.; Eisenstein, O. *Struct. Bonding (Berlin, Ger.)* **2004**, *113*, 1−36. (k) Scherer, W.; McGrady, G. S. *Angew. Chem., Int. Ed.* **2004**, *43*, 1782−1806. (l) Niu, S.; Hall, M. B. *Chem. Rev.* **2000**, *100*, 353−405. (m) Crabtree, R. H. *Angew. Chem., Int. Ed. Engl.* **1993**, *32*, 789−805. (n) Brookhart, M.; Green, M. L. H.; Wong, L. L. *Prog. Inorg. Chem.* **1988**, *36*, 1−124.

(5) (a) Dunlop-Brière, A. F.; Baird, M. C.; Budzelaar, P. H. M. *Organometallics* **2015**, *34*, 2356−2368. (b) Talarico, G.; Budzelaar, P. H. M. *Organometallics* **2014**, *33*, 5974−5982. (c) Guo, N.; Stern, C. L.; Marks, T. J. *J. Am. Chem. Soc.* **2008**, *130*, 2246−2261. (d) Grubbs, R. H.; Coates, G. W. *Acc. Chem. Res.* **1996**, *29*, 85−93.

(6) See for example: (a) Balcells, D.; Clot, E.; Eisenstein, O. *Chem. Rev.* **2010**, *110*, 749−823. (b) Häller, L. J. L.; Page, M. J.; Macgregor, S. A.; Mahon, M. F.; Whittlesey, M. K. *J. Am. Chem. Soc.* **2009**, *131*, 4604−4605. (c) Chaplin, A. B.; Poblador-Bahamonde, A. I.; Sparkes, H. A.; Howard, J. A. K.; Macgregor, S. A.; Weller, A. S. *Chem. Commun.* **2009**, 244−246. (d) Toner, A.; Matthes, J.; Gründemann, S.; Limbach, H.-H.; Chaudret, B.; Clot, E.; Sabo-Etienne, S. *Proc. Natl. Acad. Sci. U. S. A.* **2007**, *104*, 6945−6950. (e) Lersch, M.; Tilset, M. *Chem. Rev.* **2005**, *105*, 2471−2526. (f) Li, X.; Appelhans, L. N.; Faller, J. W.; Crabtree, R. H. *Organometallics* **2004**, *23*, 3378−3387. (g) Labinger, J. A.; Bercaw, J. E. *Nature* **2002**, *417*, 507−514. (h) Toner, A. J.; Gründemann, S.; Clot, E.; Limbach, H.-H.; Donnadieu, B.; Sabo-Etienne, S.; Chaudret, B. *J. Am. Chem. Soc.* **2000**, *122*, 6777−6778. (i) Shilov, A. E.; Shul'pin, G. B. *Chem. Rev.* **1997**, *97*, 2879−2932.

DOI: 10.1021/acs.organomet.6b00036
Organometallics XXXX, XXX, XXX−XXX

(7) (a) Walter, M. D.; White, P. S.; Brookhart, M. *Chem. Commun.* **2009**, 6361−6363. (b) Walter, M. D.; Moorhouse, R. A.; Urbin, S. A.; White, P. S.; Brookhart, M. *J. Am. Chem. Soc.* **2009**, *131*, 9055−9069.
(8) (a) Dunlop-Brière, A. F.; Budzelaar, P. H. M.; Baird, M. C. *Organometallics* **2012**, *31*, 1591−1594. (b) Pantazis, D. A.; McGrady, J. E.; Besora, M.; Maseras, F.; Etienne, M. *Organometallics* **2008**, *27*, 1128−1134. (c) Casey, C. P.; Tunge, J. A.; Lee, T.-Y.; Fagan, M. A. *J. Am. Chem. Soc.* **2003**, *125*, 2641−2651.
(9) Van der Eide, E. F.; Yang, P.; Bullock, R. M. *Angew. Chem., Int. Ed.* **2013**, *52*, 10190−10194.
(10) Ikeda, Y.; Takano, K.; Kodama, S.; Ishii, Y. *Chem. Commun.* **2013**, *49*, 11104−11106. (b) Sauriol, F.; Sonnenberg, J. F.; Chadder, S. J.; Dunlop-Brière, A. F.; Baird, M. C.; Budzelaar, P. H. M. *J. Am. Chem. Soc.* **2010**, *132*, 13357−13370.
(11) (a) Evans, M. E.; Li, T.; Jones, W. D. *J. Am. Chem. Soc.* **2010**, *132*, 16278−16284. (b) Steinke, T.; Shaw, B. K.; Jong, H.; Patrick, B. O.; Fryzuk, M. D.; Green, J. C. *J. Am. Chem. Soc.* **2009**, *131*, 10461−10466. (c) Ateşin, T. A.; Li, T.; Lachaize, S.; Brennessel, W. W.; García, J. J.; Jones, W. D. *J. Am. Chem. Soc.* **2007**, *129*, 7562−7569.
(12) (a) Campos, J.; Ortega-Moreno, L.; Conejero, S.; Peloso, R.; López-Serrano, J.; Maya, C.; Carmona, E. *Chem. - Eur. J.* **2015**, *21*, 8883−8896. (b) Campos, J.; Peloso, R.; Carmona, E. *Angew. Chem., Int. Ed.* **2012**, *51*, 8255−8258. (c) Crosby, S. H.; Clarkson, G. J.; Rourke, J. P. *Organometallics* **2011**, *30*, 3603−3609. (d) Rivada-Wheelaghan, O.; Donnadieu, B.; Maya, C.; Conejero, S. *Chem. - Eur. J.* **2010**, *16*, 10323−10326. (e) Frech, C. M.; Shimon, L. J. W.; Milstein, D. *Organometallics* **2009**, *28*, 1900−1908. (f) Lavallo, V.; Canac, Y.; DeHope, A.; Donnadieu, B.; Bertrand, G. *Angew. Chem., Int. Ed.* **2005**, *44*, 7236−7239. (g) Stambuli, J. P.; Incarvito, C. D.; Bühl, M.; Hartwig, J. F. *J. Am. Chem. Soc.* **2004**, *126*, 1184−1194. (h) Ingleson, M. J.; Mahon, M. F.; Weller, A. S. *Chem. Commun.* **2004**, 2398−2399. (i) Baratta, W.; Stoccoro, S.; Doppiu, A.; Herdtweck, E.; Zucca, A.; Rigo, P. *Angew. Chem., Int. Ed.* **2003**, *42*, 105−108.
(13) (a) Saßmannshausen, J. *Dalton Trans.* **2011**, *40*, 136−141. (b) Crosby, S. H.; Clarkson, G. J.; Rourke, J. P. *J. Am. Chem. Soc.* **2009**, *131*, 14142−14143. (c) Baratta, W.; Da Ros, P.; Del Zotto, A.; Sechi, A.; Zangrando, E.; Rigo, P. *Angew. Chem., Int. Ed.* **2004**, *43*, 3584−3588. (d) Baratta, W.; Mealli, C.; Herdtweck, E.; Ienco, A.; Mason, S. A.; Rigo, P. *J. Am. Chem. Soc.* **2004**, *126*, 5549−5562. (e) Baratta, W.; Herdtweck, E.; Rigo, P. *Angew. Chem., Int. Ed.* **1999**, *38*, 1629−1631. (f) Huang, D.; Streib, W. E.; Bollinger, J. C.; Caulton, K. G.; Winter, R. F.; Scheiring, T. *J. Am. Chem. Soc.* **1999**, *121*, 8087−8097. (g) Cooper, A. C.; Streib, W. E.; Eisenstein, O.; Caulton, K. G. *J. Am. Chem. Soc.* **1997**, *119*, 9069−9070.
(14) See for example: (a) Dunlop-Brière, A. F.; Baird, M. C.; Budzelaar, P. H. M. *J. Am. Chem. Soc.* **2013**, *135*, 17514−17527. (b) Findlater, M.; Cartwright-Sykes, A.; White, P. S.; Schauer, C. K.; Brookhart, M. *J. Am. Chem. Soc.* **2011**, *133*, 12274−12284 and references therein. (c) Sydora, O. L.; Kilyanek, S. M.; Jordan, R. F. *J. Am. Chem. Soc.* **2007**, *129*, 12952−12953. (d) Faller, J. W.; Fontaine, P. P. *Organometallics* **2007**, *26*, 1738−1743. (e) Chirik, P. J.; Dalleska, N. F.; Henling, L. M.; Bercaw, J. E. *Organometallics* **2005**, *24*, 2789−2794 and references therein. (f) Chirik, P. J.; Bercaw, J. E. *Organometallics* **2005**, *24*, 5407−5423. (g) Tempel, D. J.; Brookhart, M. *Organometallics* **1998**, *17*, 2290−2296. (h) Spencer, J. L.; Mhinzi, G. S. *J. Chem. Soc., Dalton Trans.* **1995**, 3819−3824. (i) Casey, C. P.; Yi, C. S. *Organometallics* **1991**, *10*, 33−35.
(15) (a) Ortuño, M. A.; Vidossich, P.; Ujaque, G.; Conejero, S.; Lledós, A. *Dalton Trans.* **2013**, *42*, 12165−12172. (b) Xu, R.; Klatt, G.; Wadepohl, H.; Köppel, H. *Inorg. Chem.* **2010**, *49*, 3289−3296 and references therein. (c) Fooladi, E.; Krapp, A.; Sekiguchi, O.; Tilset, M.; Uggerud, E. *Dalton Trans.* **2010**, *39*, 6317−6326. (d) Mitoraj, M. P.; Michalak, A.; Ziegler, T. *Organometallics* **2009**, *28*, 3727−3733. (e) Collins, S.; Ziegler, T. *Organometallics* **2007**, *26*, 6612−6623. (f) Han, Y.; Deng, L.; Ziegler, T. *J. Am. Chem. Soc.* **1997**, *119*, 5939−5945. (g) Deng, L.; Woo, T. K.; Cavallo, L.; Margl, P. M.; Ziegler, T. *J. Am. Chem. Soc.* **1997**, *119*, 6177−6186.
(16) (a) Valente, A.; Mortreux, A.; Visseaux, M.; Zinck, P. *Chem. Rev.* **2013**, *113*, 3836−3857. (b) Shiotsuki, M.; White, P. S.; Brookhart, M.; Templeton, J. L. *J. Am. Chem. Soc.* **2007**, *129*, 4058−4067. (c) Jenkins, J. C.; Brookhart, M. *J. Am. Chem. Soc.* **2004**, *126*, 5827−5842. (d) Leatherman, M. D.; Svejda, S. A.; Johnson, L. K.; Brookhart, M. *J. Am. Chem. Soc.* **2003**, *125*, 3068−3081. (e) Daugulis, O.; Brookhart, M.; White, P. S. *Organometallics* **2003**, *22*, 4699−4704. (f) Shultz, L. H.; Tempel, D. J.; Brookhart, M. *J. Am. Chem. Soc.* **2001**, *123*, 11539−11555. (g) Shultz, L. H.; Brookhart, M. *Organometallics* **2001**, *20*, 3975−3982. (h) Tempel, D. J.; Johnson, L. K.; Huff, R. L.; White, P. S.; Brookhart, M. *J. Am. Chem. Soc.* **2000**, *122*, 6686−6700. (i) Ittel, S. D.; Johnson, L. K.; Brookhart, M. *Chem. Rev.* **2000**, *100*, 1169−1203. (j) Svejda, S. A.; Johnson, L. K.; Brookhart, M. *J. Am. Chem. Soc.* **1999**, *121*, 10634−10635. (k) Johnson, L. K.; Killian, C. M.; Brookhart, M. *J. Am. Chem. Soc.* **1995**, *117*, 6414−6415. (l) Guo, Z.; Swenson, D. C.; Jordan, R. F. *Organometallics* **1994**, *13*, 1424−1432. (m) Ogasawara, M.; Saburi, M. *Organometallics* **1994**, *13*, 1911−1917. (n) Burger, B. J.; Thompson, M. E.; Cotter, W. D.; Bercaw, J. E. *J. Am. Chem. Soc.* **1990**, *112*, 1566−1577. (o) Burger, B. J.; Santarsiero, B. D.; Trimmer, M. S.; Bercaw, J. E. *J. Am. Chem. Soc.* **1988**, *110*, 3134−3146. (p) Doherty, N. M.; Bercaw, J. E. *J. Am. Chem. Soc.* **1985**, *107*, 2670−2682.
(17) (a) Conroy-Lewis, F. M.; Mole, L.; Redhouse, A. D.; Litster, S. A.; Spencer, J. L. *J. Chem. Soc., Chem. Commun.* **1991**, 1601−1603. (b) Brookhart, M.; Lincoln, D. M.; Volpe, A. F., Jr.; Schmidt, G. F. *Organometallics* **1989**, *8*, 1212−1218.
(18) (a) Ledford, J.; Shultz, C. S.; Gates, D. P.; White, P. S.; DeSimone, J. M.; Brookhart, M. *Organometallics* **2001**, *20*, 5266−5276. (b) Carr, N.; Mole, L.; Orpen, A. G.; Spencer, J. L. *J. Chem. Soc., Dalton Trans.* **1992**, 2653−2662. (c) Mole, L.; Spencer, J. L.; Carr, N.; Orpen, A. G. *Organometallics* **1991**, *10*, 49−52.
(19) (a) Pudasaini, B.; Janesko, B. G. *Organometallics* **2014**, *33*, 84−93. (b) Hasanayn, F.; Achord, P.; Braunstein, P.; Magnier, H. J.; Krogh-Jespersen, K.; Goldman, A. S. *Organometallics* **2012**, *31*, 4680−4692.
(20) Creve, S.; Oevering, H.; Coussens, B. B. *Organometallics* **1999**, *18*, 1967−1978.
(21) Roe, C. *J. Am. Chem. Soc.* **1983**, *105*, 7770−7771.
(22) (a) Brookhart, M.; Hauptman, E.; Lincoln, D. M. *J. Am. Chem. Soc.* **1992**, *114*, 10394−10401. (b) Brookhart, M.; Lincoln, D. M.; Bennett, M. A.; Pelling, S. *J. Am. Chem. Soc.* **1990**, *112*, 2691−2694. (c) Brookhart, M.; Lincoln, D. M. *J. Am. Chem. Soc.* **1988**, *110*, 8719−8720. (d) Werner, H.; Feser, R. *J. Organomet. Chem.* **1982**, *232*, 351−370. (e) Werner, H.; Feser, R. *Angew. Chem., Int. Ed. Engl.* **1979**, *18*, 157−158.
(23) (a) Pisareva, I. V.; Dolgushin, F. M.; Godovikov, I. A.; Chizhevsky, I. T. *Inorg. Chem. Commun.* **2008**, *11*, 1202−1204. (b) Hodson, B. E.; McGrath, T. D.; Stone, F. G. A. *Organometallics* **2005**, *24*, 1638−1646. (c) Speckman, D. M.; Knobler, C. B.; Hawthorne, M. F. *Organometallics* **1985**, *4*, 1692−1694.
(24) Haibach, M. C.; Wang, D. Y.; Emge, T. J.; Krogh-Jespersen, K.; Goldman, A. S. *Chem. Sci.* **2013**, *4*, 3683−3692.
(25) (a) Tejel, C.; Geer, A. M.; Jiménez, S.; López, J. A.; Ciriano, M. A. *Organometallics* **2012**, *31*, 2895−2906. (b) Turculet, L.; Feldman, J. D.; Tilley, T. D. *Organometallics* **2004**, *23*, 2488−2502.
(26) Tejel, C.; Ciriano, M. A.; Jiménez, S.; Passarelli, V.; López, J. A. *Angew. Chem., Int. Ed.* **2008**, *47*, 2093−2096.
(27) Geer, A. M.; Julián, A.; López, J. A.; Ciriano, M. A.; Tejel, C. *Chem. - Eur. J.* **2014**, *20*, 2732−2736.
(28) Geer, A. M.; Tejel, C.; López, J. A.; Ciriano, M. A. *Angew. Chem., Int. Ed.* **2014**, *53*, 5614−5618.
(29) Jiménez, S.; López, J. A.; Ciriano, M. A.; Tejel, C.; Martínez, A.; Sánchez-Delgado, R. A. *Organometallics* **2009**, *28*, 3193−3202.
(30) Tejel, C.; Ciriano, M. A.; Passarelli, V. *Chem. - Eur. J.* **2011**, *17*, 91−95.
(31) Pregosin, P. S. *NMR in Organometallic Chemistry*; Wiley-VCH: Weinheim, 2012.
(32) Fernández, I.; Martínez-Viviente, E.; Pregosin, P. S. *Inorg. Chem.* **2005**, *44*, 5509−5513.
(33) (a) Brayshaw, S. K.; Green, J. C.; Kociok-Köhn, G.; Sceats, E. L.; Weller, A. S. *Angew. Chem., Int. Ed.* **2006**, *45*, 452−456. (b) Scott, N.

DOI: 10.1021/acs.organomet.6b00036
Organometallics XXXX, XXX, XXX−XXX

M.; Dorta, R.; Stevens, E. D.; Correa, A.; Cavallo, L.; Nolan, S. P. *J. Am. Chem. Soc.* **2005**, *127*, 3516−3526.
(34) Ehlers, A. W.; Böhme, M.; Dapprich, S.; Gobbi, A.; Höllwarth, A.; Jonas, V.; Köhler, K. F.; Stegmann, R.; Veldkamp, A.; Frenking, G. *Chem. Phys. Lett.* **1993**, *208*, 111−114.
(35) The opening of the angle Rh−C^{α}−C^{β} is a consequence of the shift of the carbon C^{β} from nitrogen, from a distance of 2.639 Å (associated with an angle Rh−C^{α}−C^{β} of 104.8°, in [**3b**]$^+$) to 3.113 Å (Rh−C^{α}−C^{β} of 104.8°, in [**3c**]$^+$). Sum of van der Waals radii of C and N = 3.25 Å.
(36) Energy for agostic interactions is expected to be from modest to low (≤15 kcal mol^{-1}); see for example refs 1i, 1x, 6g, and 9.
(37) gNMR V5.0.6.0 by P. H. M. Budzelaar, published by Cherwell Scientific Publishing, Copyright 2006 Ivory soft.
(38) The sole exceptions to this general trend are the complexes [Rh(C_5Me_5)(C_2H_4)(CH_2CH_2-μ-H)]$^+$ (ref 22b) and the allyl derivative [Rh(C_5Me_5)(C_6H_9)]$^+$. Bennett, M. A.; McMahon, I. J.; Pelling, S.; Brookhart, M.; Lincoln, D. M. *Organometallics* **1992**, *11*, 127−138.

DOI: 10.1021/acs.organomet.6b00036
Organometallics XXXX, XXX, XXX−XXX